

Electric-field-driven monoclinic-to-rhombohedral transformation in $\text{Na}_{1/2}\text{Bi}_{1/2}\text{TiO}_3$

Badari Narayana Rao and Rajeev Ranjan*

Department of Materials Engineering, Indian Institute of Science, Bangalore-560012, India

(Received 31 March 2012; revised manuscript received 19 September 2012; published 4 October 2012)

The lead free ferroelectric $\text{Na}_{1/2}\text{Bi}_{1/2}\text{TiO}_3$ (NBT) is shown to exhibit electric-field-induced monoclinic (Cc) to rhombohedral ($R3c$) phase transformation at room temperature. This phenomenon has been analyzed both from the viewpoint of the intrinsic polarization rotation and adaptive phase models. In analogy with the morphotropic phase boundary systems, NBT seems to possess intrinsic competing ferroelectric instabilities near room temperature.

DOI: [10.1103/PhysRevB.86.134103](https://doi.org/10.1103/PhysRevB.86.134103)

PACS number(s): 77.80.-e, 77.22.-d, 77.80.Jk, 77.84.Cg

I. INTRODUCTION

The ferroelectric ceramic $\text{Na}_{1/2}\text{Bi}_{1/2}\text{TiO}_3$ (NBT) has been extensively investigated for its dielectric, ferroelectric, and phase transition behavior¹⁻⁵ ever since its discovery by Smolenskii *et al.* six decades ago.⁶ Though in the past two decades NBT based solid solutions have attracted considerable attention as potential lead-free piezoelectric materials,⁷⁻²⁰ the structure and phase transition behavior of the parent compound NBT is still being debated in the literature. Until recently, NBT was considered to crystallize in a rhombohedral perovskite structure (space group $R3c$) at room temperature. On heating, the rhombohedral phase was considered to transform to an intermediate tetragonal phase (space group $P4bm$) before becoming cubic ($Pm3m$).³ In the last few years this view has been challenged by high resolution synchrotron²¹⁻²³ and electron diffraction studies.^{24,25} While the room temperature structure has now been argued to possess a subtle monoclinic distortion (space group Cc), detailed electron diffraction study above room temperature have suggested that the room temperature structure transforms first into an intermediate nonpolar orthorhombic phase (space group $Pbnm$) before transforming into the tetragonal structure (space group $P4bm$). Due to the very subtle nature of the orthorhombic phase, it has not been possible to capture it in neutron/synchrotron diffraction studies. The monoclinic distortion has important significance with regard to the understanding of structure-property correlations in pure and modified NBT. Such low symmetry distortions in ferroelectric perovskites have so far been reported only in solid solutions exhibiting morphotropic phase boundary (MPB) such as PbTiO_3 - PbZrO_3 (PZT), $\text{Pb}(\text{Mg}_{1/3}\text{Nb}_{2/3})$ - PbTiO_3 (PMN-PT), and $\text{Pb}(\text{Zn}_{1/3}\text{Nb}_{2/3})$ - PbTiO_3 (PZN-PT),²⁶⁻²⁹ and not in pure ferroelectric compounds. Pure ferroelectric compounds such as BaTiO_3 , PbTiO_3 , KNbO_3 , BiFeO_3 , $\text{K}_{1/2}\text{Bi}_{1/2}\text{TiO}_3$, $\text{Pb}(\text{Mg}_{1/3}\text{Nb}_{2/3})\text{O}_3$, $\text{Pb}(\text{Zn}_{1/3}\text{Nb}_{2/3})\text{O}_3$, etc. are known to crystallize in either tetragonal or rhombohedral ground states. In this paper we highlight an interesting aspect of the low symmetry distortion in NBT by demonstrating that the monoclinic phase transforms to a high symmetry rhombohedral phase upon application of external electric field (poling). This transformation has been analyzed in the framework of two alternative theories: (i) intrinsic polarization rotation^{30,31} and (ii) the adaptive phase theory.^{32,33}

II. EXPERIMENT

NBT ceramics were prepared by the conventional solid state route. Dried oxides of high purity reagent grade Bi_2O_3 , Na_2CO_3 , and TiO_2 were used as raw materials. Stoichiometric amounts of the oxides were mixed in a planetary ball mill for 10 h with acetone as a mixing medium using zirconia bowls and balls. After drying, the mixed powders were calcined at 900 °C for 2 h in an alumina crucible. The calcined powders were then mixed with 2% PVA and pressed into pellets of 15 mm diameter and 1.5 mm thickness by uniaxial pressing at 250 MPa. These pellets were finally sintered in air at 1140 °C for 3 h. The pellets were polished to remove about 0.2 mm of the ceramic from the surface before using for any measurements. Poling was done at room temperature in silicone oil by applying a dc electrical field of 70 kV/cm for 10 min on sintered pellets. From here on, the as sintered NBT pellet which is powdered will be termed as “unpoled sample,” and the poled NBT pellet which is later crushed into powder will be termed as “poled sample.” Powder x-ray diffraction patterns were collected on the unpoled and poled samples from a Bruker powder diffractometer (model: D8 Advance) using $\text{Cu } K\alpha$ x-ray source and nickel filter. Rietveld refinement was carried out using the FullProf package.³⁴ The refined parameters include 2θ -zero, background fitted by linear interpolation, lattice parameters, atomic coordinates, thermal parameters, and the pseudo-Voigt profile shape parameters. The isotropic displacement parameters (B) showed large values for Na/Bi, and hence anisotropic displacement parameters (β_{ij}) were refined for these atoms.

III. RESULTS

Figure 1 shows the Rietveld fit of the XRD pattern of unpoled NBT powder using the two competing structural models: rhombohedral $R3c$ [Fig. 1(a)] and monoclinic Cc [Fig. 1(b)]. The goodness of fit parameter (χ^2) for the $R3c$ and Cc models were obtained as 10.1 and 5.64, respectively, suggesting an inferior overall fit with the former model. The poor fit with the $R3c$ model is noticeable even at the visual level as shown in the insets of Fig. 1(a) for two representative pseudocubic peaks $\{110\}_{pc}$ and $\{211\}_{pc}$. In contrast, the monoclinic (Cc) model could nicely account for the Bragg profiles as shown in the insets of Fig. 1(b).

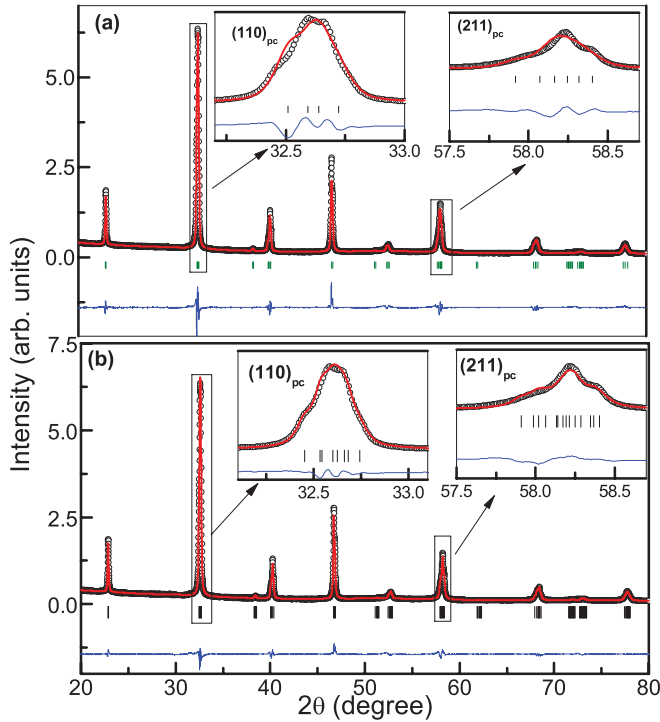


FIG. 1. (Color online) Rietveld plot of the room temperature diffraction pattern of NBT fitted with (a) rhombohedral ($R3c$) and (b) monoclinic (Cc) structural models. The open circles correspond to the observed pattern, the continuous line between the data points is the fitted pattern, and the vertical bars represent Bragg peak positions. The difference plots are shown at the bottom of the figures. For convenience, the indices in the inset are with respect to the pseudocubic cell. Every reflection appears twice due to the presence of $K\alpha_2$ component in the incident beam.

The refined parameters of the monoclinic structure (Cc) are shown in Table I. The values are in good agreement with those reported earlier by Aksel *et al.*,²² confirming the correctness of the monoclinic (Cc) structural model to fit the finer details of the observed diffraction pattern.

Figure 2 compares selected Bragg peaks of NBT before and after poling in an external electric field of 70 kV/cm. The XRD patterns were recorded on crushed powders of the poled as well as the unpoled pellets so as to rule out preferred orientation, and thereby the ambiguity that may arise in the structural analysis. It is evident from Fig. 2 that except for the pseudocubic $\{h00\}_{pc}$ type Bragg peaks, the rest of the peaks show noticeable change in the profile shapes after electric

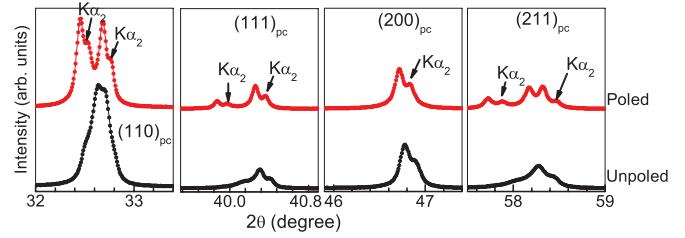


FIG. 2. (Color online) Selected pseudocubic Bragg profile electrically poled and unpoled NBT. The XRD patterns were recorded on powdered specimens.

poling. Similar results were obtained after application of a cyclic electric field confirming the irreversible nature of the transformation. Among the different peaks in the diffraction pattern, the most remarkable change in the profile shape occurs in the strongest pseudocubic reflection $\{110\}_{pc}$, which splits into a well defined doublet with nearly equal intensities. The change in the shapes of the various pseudocubic Bragg profiles after electric poling was perfectly accounted for by a rhombohedral ($R3c$) structure model as evident from the Rietveld fit shown in the insets of Fig. 3. This confirms that the monoclinic (Cc) structure is irreversibly transformed to the rhombohedral ($R3c$) structure under electric field. The refined rhombohedral structural parameters, as per the description of Megaw and Darlington,³⁵ are given in Table II. We may mention that reversing the electric field on the poled sample did not yield the monoclinic phase back. Also, the XRD pattern was found to be exactly identical when the pattern was recorded again after a month, thereby indicating that the field-transformed rhombohedral phase did not relax back to the monoclinic phase long after switching off the field. However, heating the specimen above the cubic transition temperature gave back the monoclinic phase at room temperature. It was noted that the profile shape of some of the Bragg peaks of the monoclinic phase showed diffuse and slow decaying tails which disappeared in the field stabilized rhombohedral phase. Earlier, different groups have attributed such unaccounted features in the diffraction pattern to local disorder in the monoclinic phase of NBT.^{23,36}

IV. DISCUSSION

The occurrence of monoclinic phases and electric-field-induced structural transformations are well known in ferroelectric solid solutions exhibiting MPB, as in PZN-PT and PMN-PT.^{27–29} MPB compositions exhibits

TABLE I. Monoclinic (Cc) structural parameters of unpoled NBT.

Atom	X	y	Z	B (\AA^2)
Na/Bi	0	0.25	0.0	β_{ij} (see below)
	$\beta_{11} = 0.0322(8), \beta_{22} = 0.0011(4), \beta_{33} = 0.039(1), \beta_{12} = 0.008(1), \beta_{13} = 0.0178(3), \beta_{23} = -0.011(1)$			
Ti	0.256(2)	0.248(1)	0.730(2)	0.56(7)
O1	0.004(2)	0.198(2)	0.450(2)	0.47(8)
O2	0.242(4)	0.540(2)	-0.077(4)	0.47(8)
O3	0.251(4)	-0.020(2)	-0.033(4)	0.47(8)
$a = 9.5350(2) \text{\AA}, b = 5.4789(1) \text{\AA}, c = 5.5135(1) \text{\AA}, \beta = 125.466(1)^\circ$				
$R_p = 3.25, R_{wp} = 4.74, \chi^2 = 5.64$				

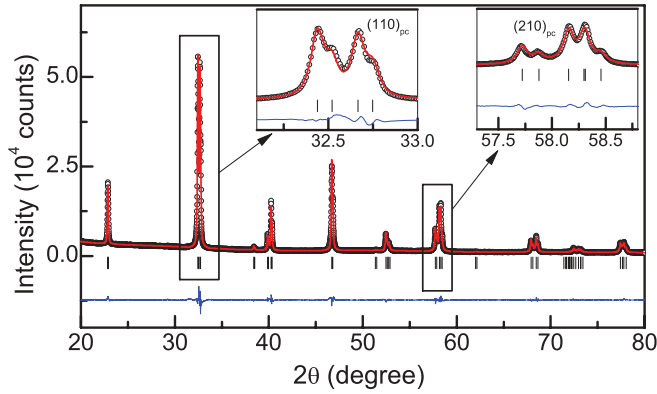


FIG. 3. (Color online) Rietveld plot of NBT after the specimen was poled at an electric field of 70 kV/cm. The observed pattern (open circles) was fitted (continuous line through the data point) with the rhombohedral ($R3c$) model. The Bragg peak positions are shown with vertical bars.

ferroelectric-ferroelectric instability at room temperature, which results in enhanced piezoelectric properties. As per the intrinsic polarization rotation theory,^{30,31} such instability is associated with the formation of a bridging monoclinic phase(s) which provide continuous low energy pathways for polarization vector to rotate on application of external electric field.^{30,31} From group theoretical considerations the monoclinic (Cc) structure of NBT can be regarded as a superposition of two independent structural distortions: (i) ferroelectric distortion with a polarization vector in the pseudocubic $(1\bar{1}0)_{pc}$ plane and (ii) octahedral tilt from any one of the types: $a^-a^-c^0$, $a^-a^-c^-$, and $a^-b^-c^-$.³⁷ If the octahedral tilt is ignored the resulting ferroelectric phase of NBT would be similar to the monoclinic structure (space group Cm) reported for the MPB composition of PZT,²⁶ the M_A or M_B phase in the notation of Vanderbilt and Cohen.³¹ The three high symmetry directions $[001]_{pc}$, $[111]_{pc}$, and $[011]_{pc}$ in the $(1\bar{1}0)_{pc}$ plane towards which, if the polarization vector rotates without leaving the plane, would lead to the formation of the tetragonal ($P4mm$), rhombohedral ($R3m$), and orthorhombic ($Amm2$) phases, respectively. The polarization vector in the monoclinic (Cc) state of the unpoled sample lies somewhere in the $(1\bar{1}0)_{pc}$ plane. The observed monoclinic to rhombohedral transformation in NBT therefore implies that the polarization vector has rotated toward the $[111]_{pc}$ direction on the $(1\bar{1}0)_{pc}$ plane, thereby causing this structural transition. This kind of low energy polarization rotation topography can in principle be manipulated by chemical modifications and other

types of monoclinic phases (such as M_C) and even triclinic phases can be in principle be stabilized.³¹

The above discussion considered the unpoled specimen to possess true monoclinic distortion. However, the observed monoclinic distortion by x-ray diffraction studies could also be due to presence of twinned rhombohedral nanodomains, which are known to cause coherent and adaptive diffraction effects.^{32,33} A detailed theoretical analysis of adaptive diffraction effects on rhombohedral structure has been performed by Wang³³ which can explain our observations equally well. As per this theory, diffraction patterns displaying seemingly monoclinic distortions are in fact originated due to the presence of twinned rhombohedral nanodomains whose dimensions are lesser than the coherence length of the x rays, leading to additional interference effects. Wang³³ has suggested that the monoclinic phase can be thought of as combination of two variants of rhombohedral nanotwins whose resultant polarization vector lies in the $(1\bar{1}0)_{pc}$ plane, and derived relations which yield the monoclinic lattice parameters. Since we are able to obtain experimentally both the high symmetry rhombohedral and the low symmetry monoclinic lattice parameters at room temperature, it becomes possible to analyze our results in the framework of the adaptive phase theory. Recent transmission electron microscopic study has shown NBT to contain a majority of $\{100\}$ type nanotwins,³⁸ which may give rise to the M_A kind of monoclinic phase. Accordingly, we made use of the relationship between the derived lattice parameters (a_m, b_m, c_m) of the monoclinic phase obtained by nanodomain averaging of the rhombohedral parameters (a_r, α_r) which is given by [Eq. (35) in Ref. 33]

$$a_m \approx \sqrt{2}a_r(1 + \frac{1}{2}\cos\alpha_r); \quad b_m = \sqrt{2}a_r\sqrt{1 - \cos\alpha_r}; \\ c_m \approx a_r.$$

It may be noted that the monoclinic (Cm) and rhombohedral ($R3m$) structures in Ref. 33 are mainly concerned with ferroelectric distortions and hence no octahedral tilt was considered. The Cc and the $R3c$ structures of NBT on the other hand consist of octahedral tilts. To adopt the formalism of Wang,³³ we therefore ignored the octahedral tilts in the structure. The Cc and the $R3c$ structures then reduced to Cm and $R3m$, respectively. A conversion of the refined hexagonal lattice parameters ($a = 5.47801 \text{ \AA}$, $c = 13.5559 \text{ \AA}$) of the $R3c$ phase (of the poled specimen) to the $R3m$ lattice parameter gives $a_r = 3.8868 \text{ \AA}$, and $\alpha_r = 89.68^\circ$. These values give the lattice parameters of the adaptive monoclinic Cm phase as $a_m = 5.5121 \text{ \AA}$, $b_m = 5.4814 \text{ \AA}$, and $c_m = 3.8868 \text{ \AA}$. Since the lattice parameters of the oblique Cc unit cell (a_c, b_c, c_c) are related to that of the Cm unit cell by $\mathbf{a}_c = \mathbf{a}_m + 2\mathbf{c}_m$, $\mathbf{b}_c = \mathbf{b}_m$, and $\mathbf{c}_c = \mathbf{a}_m$ (the bold letters denote vectors), the derived Cc lattice parameters are obtained as $a_c \sim 9.5295 \text{ \AA}$, $b_c = 5.4814 \text{ \AA}$, and $c_c = 5.5121 \text{ \AA}$. This compares very well with the experimentally obtained lattice parameter of the Cc phase using Rietveld analysis [$a = 9.5350(2) \text{ \AA}$, $b = 5.4789(1) \text{ \AA}$, $c = 5.5135(1) \text{ \AA}$, see Table I], and hence suggests the validity of the adaptive phase approach to describe the observed monoclinic like features in the diffraction pattern of NBT. From this viewpoint, the electric-field-induced monoclinic to rhombohedral transformation as seen by x-ray diffraction can be interpreted as a field-induced

TABLE II. Rhombohedral ($R3c$) structural parameters of poled NBT.

Atom	X	y	Z	$B (\text{\AA}^2)$
Na/Bi	0	0	0.27933(2)	β_{ij} (see below)
	$\beta_{11} = 0.0268(5)$, $\beta_{33} = 0.0017(4)$, $\beta_{12} = 0.0134(2)$			
Ti	0	0	0.01328(7)	1.06(5)
O	0.1223(7)	0.3416(7)	0.08330 ^a	0.71(9)
	$a = 5.47801(5) \text{ \AA}$, $c = 13.5559(1) \text{ \AA}$			
	$R_p = 2.60$, $R_{wp} = 3.84$, $\chi^2 = 3.60$			

^aO(z) fixed to deal with floating origin.

irreversible merger and growth of nano rhombohedral twins to the extent that their dimensions becomes larger than the coherence length of the x rays. For such well grown twins, the adaptive diffraction effect would no more be relevant and the compound reveals its intrinsic rhombohedral structure in the diffraction pattern. Though we are able to explain the transformation in terms of an adaptive phase approach, it does not rule out the possibility of a genuine monoclinic phase and hence the validity of the intrinsic polarization rotation theory. A careful structure analysis of the nanoregions would be required to examine the truth/falseness of the rhombohedral and monoclinic structures.

V. CONCLUSIONS

In conclusion, with the help of a simple laboratory x-ray diffraction experiment we have been able to demonstrate

the electric field driven macroscopic monoclinic (Cc) to rhombohedral ($R3c$) structural transformation in NBT. This phenomenon has been explained by both intrinsic polarization rotation-induced structure change as well as by adaptive phase theory. The true underlying mechanism can be ascertained only by detailed examination of the symmetry within the nanodomains. In view of the similarity of the features observed in the present compound and that reported for morphotropic phase boundary systems such as PMN-PT and PZN-PT, it is proposed that NBT intrinsically has competing ferroelectric-ferroelectric instability around room temperature.

ACKNOWLEDGMENT

R.R. acknowledges the financial support by the Department of Science and Technology, Government of India.

*rajeev@materials.iisc.ernet.in

- ¹I. G. Siny, C. S. Tu, and V. H. Schmidt, *Phys. Rev. B* **51**, 5659 (1995).
- ²C. S. Tu, I. G. Siny, and V. H. Schmidt, *Phys. Rev. B* **49**, 11550 (1994).
- ³G. O. Jones and P. A. Thomas, *Acta Crystallogr. Sect. B* **58**, 168 (2002).
- ⁴S. B. Vakhrushev, V. A. Isupov, B. E. Kvyatkovsky, N. M. Okuneva, I. P. Pronin, G. A. Smolenskii, and P. P. Syrnikov, *Ferroelectrics* **63**, 153 (1985).
- ⁵J. A. Zvirgzds, P. P. Kapostins, J. V. Zvirgzde, and T. V. Kruzina, *Ferroelectrics* **40**, 75 (1982).
- ⁶G. A. Smolenskii, V. A. Isupov, A. I. Agranovskaya, and N. N. Krainik, *Sov. Phys. Solid State* **2**, 2651 (1960).
- ⁷T. Takenaka, K. Maruyama, and K. Sakata, *Jpn. J. Appl. Phys. Part 1* **30**, 2236 (1991).
- ⁸Y. M. Chiang, G. W. Farrey, and A. N. Soukhovjak, *Appl. Phys. Lett.* **73**, 3683 (1998).
- ⁹Y. Hosono, K. Harada, and Y. Yamashita, *Jpn. J. Appl. Phys.* **40**, 5722 (2001).
- ¹⁰K. G. Webber, Y. Zhang, W. Jo, J. E. Daniels, and J. Rödel, *J. Appl. Phys.* **108**, 014101 (2010).
- ¹¹B. Wylie-vanEerd, D. Damjanovic, N. Klein, N. Setter, and J. Trodahl, *Phys. Rev. B* **82**, 104112 (2010).
- ¹²F. Cordero, F. Craciun, F. Trequatrini, E. Mercadelli, and C. Galassi, *Phys. Rev. B* **81**, 144124 (2010).
- ¹³C. Ma, X. Tan, E. Dul'kin, and M. Roth, *J. Appl. Phys.* **108**, 104105 (2010).
- ¹⁴J. E. Daniels, W. Jo, J. Rödel, and J. L. Jones, *Appl. Phys. Lett.* **95**, 032904 (2009).
- ¹⁵W. Jo, J. E. Daniels, J. L. Jones, X. Tan, P. A. Thomas, D. Damjanovic, and J. Rödel, *J. Appl. Phys.* **109**, 014110 (2011).
- ¹⁶O. Elkechai, M. Manier, and J. P. Mercurio, *Phys. Status Solidi A* **157**, 499 (1996).
- ¹⁷A. Sasaki, T. Chiba, Y. Mamy, and E. Otsuki, *Jpn. J. Appl. Phys.* **38**, 5564 (1999).
- ¹⁸V. A. Isupov, *Ferroelectrics* **315**, 123 (2005).
- ¹⁹J. Kreisel, A. M. Glazer, G. Jones, P. A. Thomas, L. Abello, and G. Lucazea, *J. Phys.: Condens. Matter* **12**, 3267 (2000).
- ²⁰G. O. Jones, J. Kreisel, and P. A. Thomas, *Powder Diffr.* **17**, 301 (2002).
- ²¹S. Gorfman and P. A. Thomas, *J. Appl. Crystallogr.* **43**, 1409 (2010).
- ²²E. Aksel, J. S. Forrester, J. L. Jones, P. A. Thomas, K. Page, and M. R. Suchomel, *Appl. Phys. Lett.* **98**, 152901 (2011).
- ²³E. Aksel, J. S. Forrester, B. Kowalski, J. L. Jones, and P. A. Thomas, *Appl. Phys. Lett.* **99**, 222901 (2011).
- ²⁴V. Dorcet, G. Trolliard, and P. Boullay, *Chem. Mater.* **20**, 5061 (2008).
- ²⁵G. Trolliard and V. Dorcet, *Chem. Mater.* **20**, 5074 (2008).
- ²⁶B. Noheda, D. E. Cox, G. Shirane, J. A. Gonzalo, L. E. Cross, and S.-E. Park, *Appl. Phys. Lett.* **74**, 2059 (1999).
- ²⁷B. Noheda, D. E. Cox, G. Shirane, S. E. Park, L. E. Cross, and Z. Zhong, *Phys. Rev. Lett.* **86**, 3891 (2001).
- ²⁸B. Noheda, D. E. Cox, G. Shirane, J. Gao, and Z. G. Ye, *Phys. Rev. B* **66**, 054104 (2002).
- ²⁹F. Bai, N. Wang, J. Li, D. Viehland, P. M. Gehring, G. Xu, and G. Shirane, *J. Appl. Phys.* **96**, 1620 (2004).
- ³⁰H. Fu and R. Cohen, *Nature (London)* **403**, 281 (2000).
- ³¹D. Vanderbilt and M. H. Cohen, *Phys. Rev. B* **63**, 094108 (2001).
- ³²Y. M. Jin, Y. U. Wang, A. G. Khachatryan, J. F. Li, and D. Viehland, *J. Appl. Phys.* **94**, 3629 (2003).
- ³³Y. U. Wang, *Phys. Rev. B* **76**, 024108 (2007).
- ³⁴J. Rodrigues-Carvajal, FULLPROF. A Rietveld Refinement and Pattern Matching Analysis Program, Laboratoire Leon Brillouin (CEA-CNRS) France, 2000.
- ³⁵H. D. Megaw and C. N. W. Darlington, *Acta Crystallogr. Sect. A* **31**, 161 (1975).
- ³⁶Y. Liu, L. Noren, A. J. Studer, R. L. Withers, Y. Guo, Y. Li, H. Yang, and J. Wang, *J. Solid State Chem.* **187**, 309 (2012).
- ³⁷D. M. Hatch, H. T. Stokes, R. Ranjan, Ragini, S. K. Mishra, D. Pandey, and B. J. Kennedy, *Phys. Rev. B* **65**, 212101 (2002).
- ³⁸I. Levin and I. M. Reany, *Adv. Funct. Mater.* **22**, 3445 (2012).